

# Seeing before Observable: Potential Risk Reasoning in Autonomous Driving via Vision Language Models

Jiixin Liu<sup>1\*</sup>, Xiangyu Yan<sup>2\*</sup>, Liang Peng<sup>1</sup>, Lei Yang<sup>1</sup>, Lingjun Zhang<sup>1</sup>, Yuechen Luo<sup>1</sup>, Yueming Tao<sup>1</sup>, Ashton Yu Xuan Tan<sup>1</sup>, Mu Li<sup>3</sup>, Lei Zhang<sup>3</sup>, Ziqi Zhan<sup>3</sup>, Sai Guo<sup>3</sup>, Hong Wang<sup>1</sup>, and Jun Li<sup>1</sup>

**Abstract**—Ensuring safety remains a key challenge for autonomous vehicles (AVs), especially in rare and complex scenarios. One critical but understudied aspect is the potential risk situations, where the risk is not yet observable but can be inferred from subtle precursors, such as anomalous behaviors or commonsense violations. Recognizing these precursors requires strong semantic understanding and reasoning capabilities, which are often absent in current AV systems due to the scarcity of such cases in existing driving or risk-centric datasets. Moreover, current autonomous driving accident datasets often lack annotations of the causal reasoning chains behind incidents, which are essential for identifying potential risks before they become observable. To address these gaps, we introduce PotentialRiskQA, a novel vision-language dataset designed for reasoning about potential risks prior to observation. Each sample is annotated with structured scene descriptions, semantic precursors, and inferred risk outcomes. Based on this dataset, we further propose PR-Reasoner, a vision-language-model-based framework tailored for onboard potential risk reasoning. Experimental results show that fine-tuning on PotentialRiskQA enables PR-Reasoner to significantly enhance its performance on the potential risk reasoning task compared to baseline VLMs. Together, our dataset and model provide a foundation for developing autonomous systems with improved foresight and proactive safety capabilities, moving toward more intelligent and resilient AVs.

## I. INTRODUCTION

The complexity of real driving scenarios has become one of the most significant obstacles to AV safety [1], which lies in the variety of driving scenarios, diverse kinds of traffic participants, their abundant interaction, and complicated semantic relations. Thus, accurately predicting and mitigating risks under various situations remains a challenging task. Among the various risks in driving, a particularly critical yet often overlooked challenge is the presence of **potential risks**, exemplified in Fig.1. The definition of potential risk is introduced in [2], [3] as *a kind of dangerous events, implicit events that will occur within several seconds*. In other words, it is a kind of risk that is **not directly observable** at a given moment, especially by typical autonomous vehicle (AV) systems, but with observable **precursors** and will appear soon. By properly interpreting the contextual precursors, autonomous driving systems can anticipate risks before they are fully observable, gaining more time for risk avoidance and enhancing the system’s safety redundancy.

However, such precursors are usually difficult for AV systems to recognize, as they may involve complex semantic

information, require common-sense reasoning, or be embedded in objects of information that are challenging for current perception models to detect. Current autonomous vehicle systems predominantly rely on deep neural networks for tasks like perception, planning, and end-to-end systems [1], [4], [5], whose performance is highly dependent on the quality and diversity of the training datasets. However, existing risk datasets used for training AV systems primarily emphasize observable risks, while being deficient in potential risk scenarios.

Another major defect is the lack of sufficient and comprehensive semantic annotation of existing datasets. Traditional autonomous driving datasets are often based on basic coarse annotations [6], [7], [8], failing to capture the rich contextual information necessary for identifying potential risks. In recent years, there has been a growing emergence of datasets incorporating natural language annotations [9], [10], which provide a more expressive and interpretable way to describe driving scenes or accidents. However, most of these datasets focus primarily on the basic scene descriptions, lacking a comprehensive description chain for risks, especially potential risks. Thus, such potential risk reasoning is often missing in current language-model-based AV systems due to the lack of training data that captures these subtle yet critical relationships.











To this end, we present PotentialRiskQA, a language-centric dataset for potential risk reasoning and cognition, designed to enhance autonomous vehicles’ capability to anticipate and mitigate potential risks. Specifically, we collect diverse potential risk scenarios from multiple sources and annotate each instance with a structured natural language reasoning chain that captures the causal flow from semantic precursors to inferred risks. In addition, we introduce PR-Reasoner, a VLM-based reasoning framework, which achieves state-of-the-art performance on potential risk reasoning tasks.

The main contributions of this paper are:

- We construct PotentialRiskQA, the first language-based dataset for potential risk reasoning and cognition, addressing the data sparsity and deficiency in existing autonomous driving datasets for potential risk identification challenges.
- We propose a novel annotation and reasoning paradigm for the potential risk reasoning task, featuring a structured and interpretable reasoning chain that bridges semantic precursors and inferred risks, enabling effective training of vision-language models.

\*These authors contributed equally.

<sup>1</sup> School of Vehicle and Mobility, Tsinghua University, Beijing, 100084, China

Normal Drive	Risk Precursor Appearance		Risk Appearance	Collision/Safe
<b>Case 1:</b>  $t = 0$ , normal.	 $t = 1.14s$ , the red bus is braking and $t = 3.49s$ , changing lane to right over the solid lane.	 $t = 4.38s$ , the stopping car becomes visible.	 $t = 5.73s$ , ego collides with the stopping car.	
<b>Case 2:</b>  $t = 0$ , normal.	 $t = 1.24s$ , a ball drops from the children and $t = 1.80s$ , the ball is rolling into the road.	 $t = 2.84s$ , a child rushes out for the ball.	 $t = 3.68s$ , ego stops and avoid collision.	

Base Information	Sub-task Annotation	Scene-level Annotation
<u>Risk type:</u> Blind Zone; <u>ID:</u> xxxx-xxxx-xxxx <u>Risk Precursor Appearance Frame:</u> 27 <u>Risk Appearance Frame:</u> 104 <u>Collision/Pseudo Collision Frame:</u> 136 <u>Frame per second:</u> 23.75 <u>Risk Summary:</u> The red bus ahead suddenly brakes and changes lane to right by crossing the solid line, indicating a potential risk ahead.	<u>Scenario Description:</u> road_structure: Tunnel with multiple lanes... <u>Unusual Analysis:</u> The red bus in the same lane ahead suddenly brakes... <u>Potential Risks:</u> A stopped vehicle or an obstacle ahead that is not directly visible... <u>Driving Suggestion:</u> slow down... increase the distance from the red bus ahead... <u>Meta Action:</u> SLOW DOWN AND KEEP LANE	In this scenario, the ego vehicle is driving on a straight lane in a tunnel... The behavior of bus is unusual... In normal traffic flow within a tunnel with good road conditions and no visible hazards, vehicles do not suddenly brake without warning... Possible causes could be a blocked risk source ahead of the bus that is not visible to the ego - vehicle driver, such as a stopped vehicle or an obstacle... Immediately apply gentle but firm braking to slow down... Meta action: SLOW DOWN AND KEEP LANE

Fig. 1: The structure and scenario examples of the PotentialRiskQA dataset. The key feature of potential risks is that they are not directly observable, but can be inferred from observable precursors.

- We introduce PR-Reasoner, a VLM-based reasoning framework tailored for potential risk in autonomous driving. Quantitative analysis shows its enhanced reasoning capabilities under complex driving scenarios.

## II. RELATED WORKS

### A. Potential Risk Cognition

Current research on potential risk cognition and prevention remains scarce. Early studies addressed potential risks through predefined rules and knowledge, with a scenario-knowledge matching method. A typical early study is [2], [3], which built a knowledge base for the case of a child possibly running across the street to catch a bus. A more recent promising line lies in knowledge-graph-based methods [11], [12], leveraging knowledge graph (KG) embedding techniques to encode natural language KG into vectors, followed by scene graph construction and match methods [13], [14]. However, such methods heavily rely on the richness of manually crafted knowledge bases, which is inherently against the long-tail feature of driving scenarios.

With the development of deep learning, more studies have adopted neural networks to perform risk anticipation tasks by such as visual feature analysis [15], [16], trajectory prediction [17], [18], risk zone estimation [19], etc. However, the performance of data-driven methods is restricted by the training dataset, while the potential risk problem remains an underexplored issue with the long-tail feature and a lack of expression in current datasets.

In general, extensive knowledge of potential risks and sufficient data both play a crucial role in potential risk cognition tasks. The rapidly advancing Vision-Language Models (VLMs) and Multimodal Large Language Models (MLLMs)

[20], [21], [22], [23] have shown great potential due to their knowledge acquired from extensive training corpora and their learning capabilities from datasets [24]. Therefore, a language-based dataset specifically focused on potential risks in autonomous driving is more necessary.

### B. Risk-Centric Datasets for Autonomous Driving

Over the past few years, a number of risk-oriented datasets have been introduced to supplement traditional AD datasets like Waymo [25] or nuScenes [6]. Despite recent progress, existing risk-centric datasets are not sufficient for potential risk anticipation, falling short in several key aspects.

Identifying potential risks requires temporally coherent, first-person sequential data to capture semantic precursors before any observable danger. However, many risk-centric datasets adopt third-person or aerial views [26], [27], [28], or provide only isolated snapshots of the risk moment [10], [29], lacking sufficient temporal context for forward inference. Even in video-based datasets with continuous sequences [9], potential risk scenarios account for only a small fraction, as these datasets usually target all types of risk. This imbalance further limits the ability of VLMs to effectively learn from early precursors and anticipate potential risks.

Besides, they lack structured, language-based annotations that connect semantic precursors to risks, which is an essential form of supervision for training VLMs. Early accident datasets usually provide only coarse annotations [30], e.g., bounding boxes, object types, or high-level enumerable event tags, but lack the semantic depth. In recent years, with the rise of VLMs, a large number of accident or driving risk datasets annotated with natural language have begun to

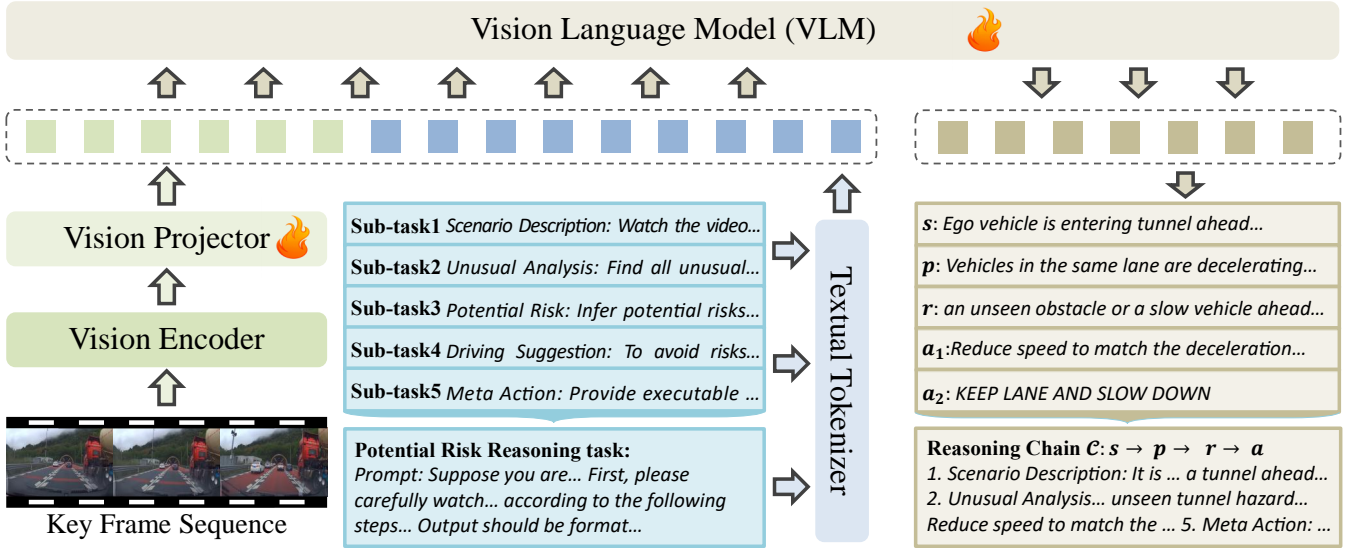


Fig. 2: The proposed PR-Reasoner framework. Based on VLMs, the proposed model takes a frame sequence and textual prompts as inputs. The output is a structured reasoning chain.

emerge, either simple risk descriptions [9], [10] or multiple risk-related sub-tasks and QA-pairs [31], [32].

To our knowledge, the only prior dataset specifically addressing potential risks is proposed in [3]. However, this dataset is limited in scale, lacks rich annotations for reasoning, and is not publicly available.

### III. METHODOLOGY

#### A. Overview of PR-Reasoner

We formalize the potential risk reasoning task as follows. Given the visual observation  $V_t$  and textual context  $T_t$  at current time step  $t$ , the goal is to infer the potential risk  $r$  that is not currently observable, but may emerge after a future interval  $\Delta t$  based on identifiable semantic precursors  $p$  in the current input. Formally, we define a reasoning model  $f_r$ , s.t.,

$$r = f_r(T_t, V_t) \quad (1)$$

where  $p \in T_t \cup V_t$ ,  $r \notin T_t \cup V_t$ , but  $r \in T_{t+\Delta t} \cup V_{t+\Delta t}$ .

To solve this task, we propose PR-Reasoner, a vision-language reasoning framework built upon a VLM backbone, as shown in Fig.2. The PR-Reasoner framework comprises a vision encoder, a textual tokenizer, and a VLM backbone. Additionally, it incorporates a structured reasoning chain that guides both the prompt formulation and output generation, enabling logical and interpretable potential risk reasoning.

In this framework, the input text and visual information are first encoded as token sequences  $X_T$  and  $X_V$ , respectively, which are then concatenated and fed into the VLM:

$$\mathcal{C} = \text{VLM}(X_T, X_V) \quad (2)$$

The output  $\mathcal{C}$  is the structured reasoning chain, which captures the intermediate inference process from scene understanding to actionable decisions. Specifically, it begins with a semantic description  $s$ , identifies the precursor  $p$ ,

infers the latent risk  $r$ , and proposes a driving suggestion  $a$ :

$$\mathcal{C} : s \rightarrow p \rightarrow r \rightarrow a \quad (3)$$

1) *Vision Encoder*: Considering the limitations of the context window and onboard deployment demands, we sample every 0.5 seconds in the backward direction before the current time step  $t$ , resulting in a total of 5 frames that cover a 2-second time window. Our later analysis demonstrates that this window length is enough for most potential risk scenarios. Each frame will be resized to a specific resolution  $H \times W$ , constructing a structured visual input  $V_t \in \mathbb{R}^{N \times H \times W \times 3}$ .  $N$  denotes the number of frames, and  $N = 5$  for most scenarios. However, in our datasets, due to limitations in data duration, the value of  $N$  may be a smaller value.

Given the visual input  $V_t$ , we first extract visual features using the default vision encoder provided by different VLM backbones. These features are then transformed into modality-aligned visual tokens  $X_V$  via a trainable visual projection layer, ensuring compatibility with the language input space.

2) *Textual Tokenizer*: The textual tokenizer transforms raw language inputs  $T_t$  into token sequences  $X_T$  suitable for processing by the VLM backbone, and subsequently decodes the output tokens into natural language. In this work, we adopt the default tokenizer provided by each selected VLM backbone to ensure compatibility and consistent text encoding behavior across models.

3) *VLM Backbones*: To evaluate the generality and effectiveness of our method across different architectures and model capacities, we adopted a diverse set of VLM backbones in this work. The VLM backbone receives the concatenated visual and textual tokens  $(X_V, X_T)$  as input and generates the corresponding output tokens in an autoregressive manner. The output tokens are then decoded by the

textual tokenizer to produce the final textual reasoning chain  $\mathcal{C}$ .

### B. Reasoning Chain with Auxiliary Sub-tasks

To support interpretable and semantically grounded reasoning in the potential risk reasoning task, we introduce a structured reasoning chain paradigm  $\mathcal{C}$  for VLMs. The reasoning chain consists of five progressive components: (1) a high-level scene description ( $s$ ), (2) identification of a semantic risk precursor ( $p$ ), (3) inference of the potential risk ( $r$ ), (4) a driving suggestion to avoid risk ( $a_1$ ), and (5) a meta-action executable and compatible with current AV systems ( $a_2$ ).

This chain reflects how humans reason about potential risks in complex driving environments. To effectively learn this structured reasoning process, we further propose five auxiliary sub-tasks, each aligned with a specific component of the chain, to provide targeted supervision and enhance reasoning capability, including *Scenario Description*, *Unusual Analysis*, *Potential Risks*, *Driving Suggestion*, and *Meta Action*. By learning from such auxiliary sub-tasks, PR-Reasoner can acquire the ability to reason about potential risks in complex and ambiguous scenarios, grounding its decisions in interpretable and context-aware semantic cues. The detailed definition of these sub-tasks can be found in the Supplementary Material.

## IV. POTENTIALRISKQA DATASET

### A. Dataset Overview

We provide PotentialRiskQA, a language-based dataset for the potential risk reasoning task. From multiple sources, we collected first-person perspective videos related to potential risks during driving, most of which were sourced from in-vehicle dash cameras. Fig.1 illustrates the structure with the task hierarchy of the dataset, where three parts of annotations are provided for each risk scenario, i.e., base information, scene-level annotation, and sub-task annotation.

The base information includes the risk type and ID, key frame annotations, and a brief risk summary. The key frame annotations identify three critical moments in the video. The **Precursor Appearance Frame** marks the earliest time when the semantic precursors become observable to the ego vehicle, allowing the potential risk to be inferred, e.g., other traffic participants' unexpected behaviors, unusual signals, etc. The **Risk Appearance Frame** corresponds to the moment when the risk becomes observable and should be detected by AV system. Finally, the (Pseudo) **Collision Frame** denotes either the point of collision. Under near-collision conditions, this marks the most critical frame at which a collision would have occurred if the ego vehicle executed no evasive maneuver.

The scene-level annotation is directly aligned with the reasoning chain  $\mathcal{C}$  required for potential risk reasoning. As aforementioned, this part of annotation consists of five progressive components. These components collectively span the reasoning process from scene understanding to risk anticipation and action planning. Furthermore, the sub-task

annotations, aligned with the auxiliary sub-tasks, provide more detailed information about the scenarios and are in a more structured format.

### B. Dataset Statistics

The dataset currently comprises 400 potential risk scenarios, annotated with 2,400 vision-language QA pairs and nearly 80,000 keyframes, spanning a diverse range of driving conditions, road structures, and traffic participants, shown in Fig.3d-f. Moreover, the dataset is continuously expanding as we actively collect and annotate new potential risk instances. We categorized the potential risk scenarios in the dataset and ultimately identified nine categories, covering a wide range of commonly encountered yet potentially unsafe traffic scenarios, shown in Fig.3a. The most frequent categories are *Blind Zone (BZ)* and *Sudden Behavior (SB)*, which correspond to the two representative scenario types in Fig.1.

To further investigate the temporal characteristics of potential risk events, we analyze two key time intervals in each scenario: (1) the duration from Precursor Appearance to Collision (Precursor-to-Collision), and (2) the duration from Risk Appearance to Collision (Risk-to-Collision), as illustrated in Fig. 3b. The results reveal that over 50% of Risk-to-Collision intervals are shorter than 1.5 seconds, highlighting the difficulty of avoiding such risks simply by reacting after the risks become observable. In contrast, the Precursor-to-Collision interval exhibits a broader distribution, with a median duration of approximately 2.9 seconds, almost twice that of the Risk-to-Collision interval (1.45 seconds). This extended temporal window proves the value of identifying semantic precursors, which provide ADS with critical lead time for risk mitigation.

Fig. 3c further quantifies the additional mitigation time gained by detecting precursors instead of observable risks (Precursor-to-risk). The median gain is 1.50 seconds, indicating a substantial temporal advantage that can be leveraged for safer and more proactive decision-making. Together, these findings emphasize the importance of precursor identification and potential risk reasoning in semantically complex scenarios. This enables the AV system to gain more lead time for risk mitigation, allowing it to proactively respond to hazards in advance, thereby avoiding entry into high-risk operational domains of reactive modules such as AEB, and ultimately enhancing the safety of AV.

### C. Dataset Construction

*1) Data Collection:* To construct the dataset, we curated driving videos and scenarios from three primary sources: public accident videos, driving accident datasets, and real-vehicle collected data.

**Public accident videos:** We sourced publicly available driving and accident videos from online platforms, e.g., YouTube and Bilibili. These videos are valuable because they capture real-world, uncontrolled conditions, including rare and unpredictable driving behaviors. We manually screened a large volume of videos and extracted short clips that include potential-risk-related incidents or near-collision events.

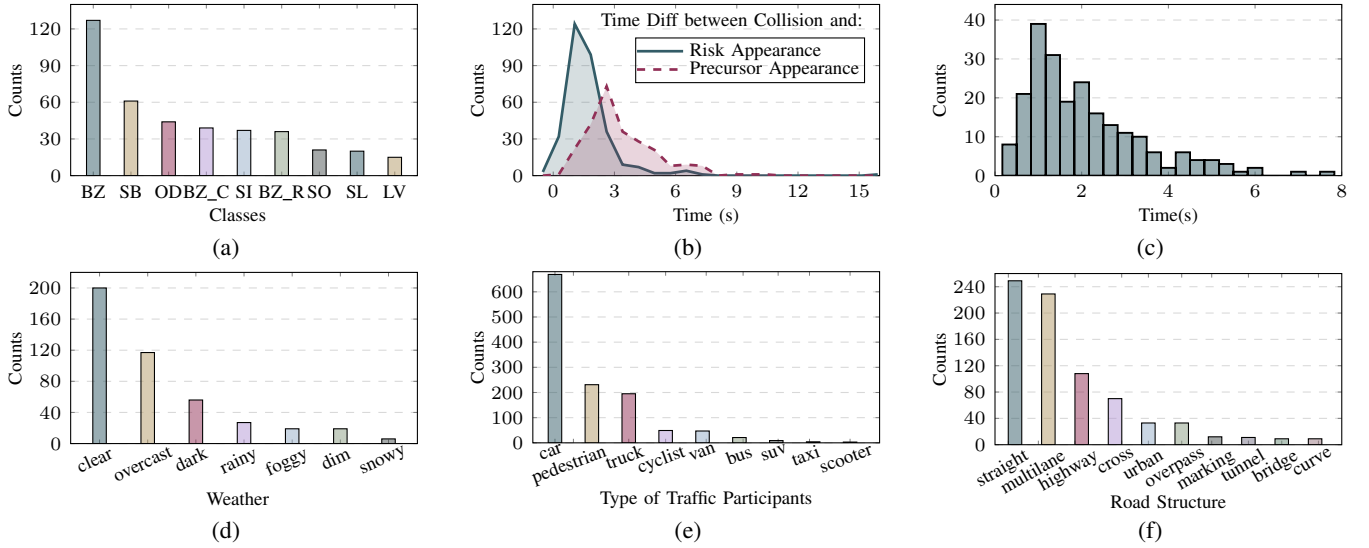


Fig. 3: Dataset statistics of PotentialRiskQA dataset: (a) The count of different risk categories. The detailed definition of the categories can be found in the Supplementary. (b) The comparison of *Risk to Collision* time and *Precursor to Collision* time. (c) The distribution of the additional risk mitigation time earned by indication precursors. (d-f) The count of different (d) weather; (e) types of traffic participants; (f) road structure in the dataset.

**Driving accident datasets:** We prioritized datasets that provide video clips or frame sequences, e.g., DrivingDojo [33], DADA-2000 [9], and CAP [34], instead of isolated snapshots at the accident moment. For these datasets, we conducted an initial auto-filtering based on specific rules according to their annotation contents, followed by further manual filtering. The selected clips are further converted into a unified format that is consistent with our annotation pipeline.

**Real-vehicle collected data:** In addition to the public datasets, several scenario data were collected using real vehicles in the test field. In detail, we selected several representative scenarios during the mining of public datasets and reproduced them in the test field. Data collection was conducted using an onboard front-facing camera, which features a 121° FOV, 1080p resolution, and a 2.8 mm focal length.

2) *Auto Annotation:* We use an LLM-based auto-annotate framework to generate the language-based annotations. For each sub-task, we adopt a multi-agent annotation procedure consisting of four stages: First, a *Base Annotation* is generated using both the image input and prompts, along with the outputs from previous sub-tasks to maintain consistency across the reasoning chain. Next, a *Content Checking* step evaluates the alignment between the scenario and the base annotation, identifies unsupported, missed, or inaccurate statements, and produces revision suggestions. Then, in the *Validation&Merging* stage, these revisions are reviewed against the video context and merged with the base annotations to form the final result. This step also standardizes the output into a unified format for each sub-task. Finally, *Manual Inspection* is applied to ensure the accuracy and consistency of the annotations.

For the scene-level stage, the same four-stage annotation procedure is applied, while each sub-task will be used in the *Content Checking* part. By employing different agents at various stages, we can reduce the bias introduced by a single LLM model, thereby enhancing the quality of dataset annotations [35]. Specifically, in this work, we use doubao1.5-vision from ByteDance [36], Qwen2.5-VL from Ali [22], and GPT4o from OpenAI [21] as the annotation agents.

## V. EXPERIMENTS

### A. Evaluation Metrics

To evaluate the potential risk reasoning and cognition capabilities of MLLMs, we propose a benchmark based on the PotentialRiskQA dataset. Specifically, we employ two types of evaluation metrics: the first involves traditional standard NLP metrics to assess the semantic similarity between model responses and the ground-truth annotations. In detail, following [10], we choose BLEU-1 (BL-1), BLEU-4 (BL-4), ROUGE-L (RO), METEOR (ME), CIDEr (CI), BertScore-F1 (BS), and BleuRT (BR) as metrics to evaluate the language similarity between predictions from multiple aspects, such as words, phrases, and sentence structures.

In the second part, we deployed LLM-scores, which use MLLMs with a strong ability to judge the quality of the answers. Following [29], [37], [38], we design three criteria for the LLM scorer to judge the quality of the answers: correctness, comparison, and consistency.

**Correctness (CORR):** This criterion assesses whether the answer is correct to the sub-task. The LLM scorer evaluates the alignment between the scenario and the answer based on the scenario images and assigns a correctness score.



VLMs	Size (B)	NLP scores							LLM scores		
		BL-4	BL-1	ME	RO	CI	BS	BR	CORR	COMP	CONS
Baseline (Open-Source Pretrained VLMs)											
Baseline-SmolVLM2-256M	0.25B	0.00	0.07	0.08	0.09	0.002	0.61	0.30	0.04	<b>0.02</b>	0.00
Baseline-SmolVLM2-500M	0.5B	0.01	0.20	0.14	0.12	0.005	0.63	0.35	0.03	0.01	0.01
Baseline-llava-ov-0.5b	0.9B	<b>0.17</b>	<b>0.35</b>	<b>0.27</b>	<b>0.18</b>	<b>0.021</b>	<b>0.72</b>	<b>0.36</b>	0.08	0.01	0.07
Baseline-DS-vl2-tiny (MoE)	1.0B	0.04	0.15	0.13	0.11	0.011	0.63	0.28	<b>0.16</b>	0.01	<b>0.08</b>
Baseline-SmolVLM2-2.2B	2.2B	0.02	0.13	0.12	0.12	0.010	0.64	0.37	0.12	0.03	0.06
Baseline-DS-vl2-small (MoE)	2.8B	0.26	0.46	0.30	0.23	0.046	0.74	0.39	0.39	0.07	0.31
Baseline-Qwen2.5-VL-3B	3.4B	<b>0.28</b>	<b>0.47</b>	<b>0.32</b>	<b>0.30</b>	<b>0.121</b>	<b>0.78</b>	<b>0.45</b>	<b>0.49</b>	<b>0.09</b>	<b>0.33</b>
Baseline-Qwen2.5-Omni-3B	3.4B	0.22	0.36	0.26	0.24	0.042	0.76	0.41	0.35	0.04	0.23
Baseline-llava-v1.6-7b	7.6B	0.22	0.41	<b>0.36</b>	0.24	0.046	0.75	0.42	0.41	0.07	0.33
Baseline-llava-ov-7b	8.0B	0.23	0.42	0.35	0.26	0.086	0.76	0.43	0.48	0.10	0.36
Baseline-Qwen2.5-VL-7B	8.3B	0.25	0.40	0.31	<b>0.32</b>	<b>0.095</b>	<b>0.79</b>	<b>0.47</b>	<b>0.66</b>	<b>0.22</b>	<b>0.42</b>
Baseline-Qwen2.5-Omni-7B	10.7B	<b>0.28</b>	<b>0.47</b>	0.31	0.28	0.053	0.77	0.40	0.47	0.10	0.34
Ours (PR-Reasoner with different VLM backbones)											
PR-SmolVLM2-256M	0.25B	0.38	0.56	<b>0.55</b>	0.37	0.209	<b>0.82</b>	0.51	0.36	0.05	0.29
PR-SmolVLM2-500M	0.5B	0.37	0.60	0.52	0.36	0.282	0.81	0.50	0.48	0.10	0.35
PR-llava-ov-0.5b	0.9B	0.39	0.60	<b>0.55</b>	<b>0.40</b>	<b>0.339</b>	<b>0.82</b>	<b>0.52</b>	<b>0.60</b>	<b>0.23</b>	<b>0.45</b>
PR-DS-vl2-tiny (MoE)	1.0B	<b>0.41</b>	<b>0.63</b>	<b>0.55</b>	<b>0.40</b>	0.337	<b>0.82</b>	<b>0.52</b>	0.57	0.21	<b>0.45</b>
PR-SmolVLM2-2.2B	2.2B	0.38	0.59	0.52	0.38	0.240	0.82	0.52	0.64	0.23	0.45
PR-DS-vl2-small (MoE)	2.8B	0.42	0.64	0.55	0.42	0.334	<b>0.83</b>	0.53	0.70	0.35	0.50
PR-Qwen2.5-VL-3B	3.4B	0.40	0.62	0.54	0.42	0.343	<b>0.83</b>	0.53	<b>0.74</b>	<b>0.36</b>	0.51
PR-Qwen2.5-Omni-3B	3.4B	<b>0.44</b>	<b>0.65</b>	<b>0.57</b>	<b>0.54</b>	<b>0.421</b>	<b>0.83</b>	<b>0.54</b>	0.72	<b>0.36</b>	<b>0.53</b>
PR-llava-v1.6-7b	7.6B	<b>0.44</b>	<b>0.65</b>	0.56	<b>0.43</b>	0.363	<b>0.83</b>	<b>0.54</b>	0.74	0.36	0.52
PR-llava-ov-7b	8.0B	0.39	0.59	<b>0.57</b>	0.42	<b>0.425</b>	<b>0.83</b>	0.53	0.72	0.35	0.51
PR-Qwen2.5-VL-7B	8.3B	0.41	0.62	0.54	0.42	0.307	<b>0.83</b>	0.53	<b>0.75</b>	<b>0.39</b>	<b>0.53</b>
PR-Qwen2.5-Omni-7B	10.7B	0.40	0.61	<b>0.57</b>	0.42	0.398	<b>0.83</b>	<b>0.54</b>	0.70	0.36	<b>0.53</b>

TABLE I: Evaluation results of pre-trained VLMs, as well as the proposed method PR-Reasoner with different VLM backbones. By injecting the reasoning chain paradigm into the VLMs via SFT, these models show improved performance in the potential risk reasoning task. Notably, to avoid confusion, we use the number of parameters marked in the official repository on HuggingFace. For Mixture-of-Expert (MoE) architecture models, the parameter number is the number of activated parameters. The best performance of each scale is reported in bold.

**Comparison (COMP):** This criterion uses the LLM scorer to compare the quality of the answer and the annotation (label). The position bias [37] is facilitated by getting two scores with different orders of the two answers, and using their average as the final comparison score.

**Consistency (CONS):** This criterion aims to assess the consistency between the model’s responses and the predefined annotations. This metric directly reflects the effectiveness of fine-tuning.

Finally, all LLM scores are normalized to the range of 0 to 1, where a higher score indicates better answer quality. We used Gemini-2.5-pro as the LLM scorer, which is one of the most advanced models nowadays, and is not used in either the annotation stage or the evaluation stage. For different sub-tasks, we prompt the LLM scorer to focus on different aspects. For example, the accuracy of object recognition in *scenario description*, the plausibility of reasoning in *potential risks*, and the safety and executability of suggestions in *driving suggestion*.

## B. Experimental Setup

1) *Model Selection:* Considering the real-time requirements and computational constraints of onboard deployment, we focus on lightweight VLMs with no more than around 7B parameters. Specifically, we select several representative VLMs around three scales: less than 1B (small), around 3B (medium), and around 7B (large), from Qwen [22], Deepseek (DS) [23], LLaVA [39], and HuggingFace [40]. These mod-

els have demonstrated strong performance in vision-language reasoning tasks while maintaining reasonable computational demands for onboard use. In comparison, we first evaluate the performance of the pre-trained models on the potential risk reasoning task. Then, we applied the PR-Reasoner framework, by injecting the proposed reasoning paradigm  $\mathcal{C}$  in these models via supervised fine-tuning (SFT) on these models.

2) *Implement Details:* We split the total of 400 scenarios into training, validation, and test sets in a ratio of 75:10:15. Each scenario contains 5 sub-tasks with a scene-level task, total of 6 multimodal QA-pairs. We conducted LoRA-SFT with an initial learning rate of  $1e-4$ , mainly based on the ms-swift framework [41]. The training process is applied on Nvidia H20 GPUs with 96GB of memory, with 4 epochs trained for each model.

To ensure the reproducibility of the experiment, we use the same prompt as the *Base Annotation* part in the auto-annotation procedure. Besides, we employed greedy decoding during inference, selecting the highest-probability token at each step to generate outputs, thereby eliminating randomness in the decoding process. We selected the best model on the validation dataset using the early stop strategy with the default Causal Loss as the metric.

## C. Results and Analysis

1) *Effect of PR-Reasoner Framework:* As shown in Table.I, it is evident that introducing the proposed PR-

Reasoner framework significantly enhances model performance on the potential risk reasoning task over various VLM backbones. This improvement is particularly noticeable for small- and medium-sized models, e.g., the SmolVLM2 models. For large-scale pre-trained VLMs that already possess strong reasoning capabilities, the proposed method also provides performance improvements across the metrics.

Overall, by introducing PR-Reasoner, VLMs exhibit significant improvements in both the accuracy and reliability of their responses on the potential risk reasoning task, as well as in the completeness of their structured reasoning paths. This enables the models not only to identify risks and provide decision recommendations accurately, but also to produce structured outputs that are compatible with existing AV systems, thereby effectively enhancing the overall safety of autonomous driving.

2) *Effect of Model Scales*: We further analyze the impact of model size on the performance of the potential risk reasoning task. For pre-trained VLMs, there exists a clear positive correlation between model size and task performance across both NLP and LLM metrics. However, by introducing the reasoning paradigm of PR-Reasoner, this scaling effect diminishes significantly beyond 3B parameters. Models around 3B, such as Qwen2.5-VL-3B, already achieve competitive performance across most metrics. Further increasing the parameter count to large scale yields marginal improvements, particularly in LLM scores. This observation suggests that the proposed reasoning chain paradigm introduced by PR-Reasoner compensates for the lack of scale, enabling smaller models to match the similar reasoning ability of larger models in the potential risk reasoning task.

VLMs	CORR	COMP	CONS
Baseline-llava-ov-0.5b	0.03	0.01	0.05
Baseline-Qwen2.5-Omni-3B	0.11	0.00	0.11
Baseline-Qwen2.5-VL-7B	0.40	0.07	0.26
PR-llava-ov-0.5b	0.42	0.14	0.24
PR-Qwen2.5-Omni-3B	0.59	0.22	0.32
PR-Qwen2.5-VL-7B	0.66	0.27	0.37

TABLE II: The performance of representative models in potential risk reasoning tasks.

3) *Performance on Potential Risk Reasoning Task*: Specifically, we evaluate the effectiveness of the proposed PR-Reasoner with several representative VLM backbones on the potential risk reasoning task, focusing solely on scene-level annotations, as shown in Table II. The performance trends observed here largely align with those seen across all tasks on average, supporting the overall conclusions regarding model behavior.

Notably, the impact of model scale is more pronounced on this task compared to the average of all tasks, even beyond 3B parameters, indicating that larger models benefit more when handling complex, multi-step reasoning without the saturation observed in overall task metrics. Moreover, the average performance on this task is consistently lower than the overall task average. These observations are consistent with the nature of the potential risk reasoning task, which

inherently involves longer and more complex reasoning chains.

## VI. CONCLUSION

We present PotentialRiskQA, the first language-based dataset specifically designed for potential risk reasoning in autonomous driving systems, capturing hundreds of multi-source, real-world potential risk scenarios under complex driving conditions, with nearly 80,000 annotated frames. To support this task, we propose a novel annotation and reasoning paradigm centered around a structured reasoning chain, which bridges semantic precursors with potential risks through five aligned sub-tasks. Building on this foundation, we introduce PR-Reasoner, a VLM-based framework tailored for potential risk reasoning. We evaluate PR-Reasoner alongside several state-of-the-art VLMs with onboard-scale model sizes, and the results demonstrate its superior performance in handling potential risk reasoning under challenging scenarios. We believe this work provides an essential foundation for improving the semantic foresight and proactive safety capabilities of autonomous driving systems, facilitating existing performance limitations in complex, unstructured environments.

## REFERENCES

- [1] L. Peng, B. Li, W. Yu, K. Yang, W. Shao, and H. Wang, "Sotif entropy: Online sotif risk quantification and mitigation for autonomous driving," *IEEE Transactions on Intelligent Transportation Systems*, vol. 25, no. 2, pp. 1530–1546, 2023.
- [2] A. D. Lattner, I. J. Timm, M. Lorenz, and O. Herzog, "Knowledge-based risk assessment for intelligent vehicles," in *International Conference on Integration of Knowledge Intensive Multi-Agent Systems*, 2005. IEEE, 2005, pp. 191–196.
- [3] R. Takahashi, N. Inoue, Y. Kuriya, S. Kobayashi, and K. Inui, "Explaining potential risks in traffic scenes by combining logical inference and physical simulation," *International Journal of Machine Learning and Computing*, vol. 6, no. 5, p. 248, 2016.
- [4] J. Liu, H. Wang, Z. Cao, W. Yu, C. Zhao, D. Zhao, D. Yang, and J. Li, "Semantic traffic law adaptive decision-making for self-driving vehicles," *IEEE Transactions on Intelligent Transportation Systems*, vol. 24, no. 12, pp. 14 858–14 872, 2023.
- [5] W. Sun, X. Lin, Y. Shi, C. Zhang, H. Wu, and S. Zheng, "Sparsedrive: End-to-end autonomous driving via sparse scene representation," *arXiv preprint arXiv:2405.19620*, 2024.
- [6] H. Caesar, V. Bankiti, A. H. Lang, S. Vora, V. E. Liong, Q. Xu, A. Krishnan, Y. Pan, G. Baldan, and O. Beijbom, "nusenes: A multimodal dataset for autonomous driving," in *CVPR*, 2020.
- [7] X. Zhang, L. Wang, J. Chen, C. Fang, G. Yang, Y. Wang, L. Yang, Z. Song, L. Liu, X. Zhang *et al.*, "Dual radar: A multi-modal dataset with dual 4d radar for autonomous driving," *Scientific Data*, vol. 12, no. 1, p. 439, 2025.
- [8] T. Xie, Z. Song, F. Wen, J. Li, G. Liu, and Z. Zhao, "Truckv2x: A truck-centered perception dataset," 2025. [Online]. Available: <https://arxiv.org/abs/2507.09505>
- [9] J. Fang, D. Yan, J. Qiao, J. Xue, and H. Yu, "Dada: Driver attention prediction in driving accident scenarios," *IEEE transactions on intelligent transportation systems*, vol. 23, no. 6, pp. 4959–4971, 2021.
- [10] S. Malla, C. Choi, I. Dwivedi, J. H. Choi, and J. Li, "Drama: Joint risk localization and captioning in driving," in *Proceedings of the IEEE/CVF winter conference on applications of computer vision*, 2023, pp. 1043–1052.
- [11] X. Li, J. Liu, J. Li, W. Yu, Z. Cao, S. Qiu, J. Hu, H. Wang, and X. Jiao, "Graph structure-based implicit risk reasoning for long-tail scenarios of automated driving," in *2023 4th International Conference on Big Data, Artificial Intelligence and Internet of Things Engineering (ICBAIE)*. IEEE, 2023, pp. 415–420.

- [12] J. Cao, J. Fang, Z. Meng, and S. Liang, "Knowledge graph embedding: A survey from the perspective of representation spaces," *ACM Computing Surveys*, vol. 56, no. 6, pp. 1–42, 2024.
- [13] R. Wickramarachchi, C. Henson, and A. Sheth, "Knowledge graphs of driving scenes to empower the emerging capabilities of neurosymbolic ai," *IEEE Internet Computing*, vol. 28, no. 6, pp. 62–67, 2025.
- [14] C. Lv, M. Qi, L. Liu, and H. Ma, "T2sg: Traffic topology scene graph for topology reasoning in autonomous driving," *arXiv preprint arXiv:2411.18894*, 2024.
- [15] Y. Yao, M. Xu, Y. Wang, D. J. Crandall, and E. M. Atkins, "Unsupervised traffic accident detection in first-person videos," in *2019 IEEE/RSJ International Conference on Intelligent Robots and Systems (IROS)*. IEEE, 2019, pp. 273–280.
- [16] J. Fang, J. Qiao, J. Bai, H. Yu, and J. Xue, "Traffic accident detection via self-supervised consistency learning in driving scenarios," *IEEE Transactions on Intelligent Transportation Systems*, vol. 23, no. 7, pp. 9601–9614, 2022.
- [17] Z. Shan, Q. Zhu, and D. Zhao, "Vehicle collision risk estimation based on rgb-d camera for urban road," *Multimedia systems*, vol. 23, pp. 119–127, 2017.
- [18] W. Hu, X. Xiao, D. Xie, and T. Tan, "Traffic accident prediction using vehicle tracking and trajectory analysis," in *Proceedings of the 2003 IEEE International Conference on Intelligent Transportation Systems*, vol. 1. IEEE, 2003, pp. 220–225.
- [19] K.-H. Zeng, S.-H. Chou, F.-H. Chan, J. Carlos Niebles, and M. Sun, "Agent-centric risk assessment: Accident anticipation and risky region localization," in *Proceedings of the IEEE Conference on Computer Vision and Pattern Recognition*, 2017, pp. 2222–2230.
- [20] J. Achiam, S. Adler, S. Agarwal, L. Ahmad, I. Akkaya, F. L. Aleman, D. Almeida, J. Altenschmidt, S. Altman, S. Anadkat *et al.*, "Gpt-4 technical report," *arXiv preprint arXiv:2303.08774*, 2023.
- [21] A. Hurst, A. Lerer, A. P. Goucher, A. Perelman, A. Ramesh, A. Clark, A. Ostrow, A. Welihinda, A. Hayes, A. Radford *et al.*, "Gpt-4o system card," *arXiv preprint arXiv:2410.21276*, 2024.
- [22] S. Bai, K. Chen, X. Liu, J. Wang, W. Ge, S. Song, K. Dang, P. Wang, S. Wang, J. Tang, H. Zhong, Y. Zhu, M. Yang, Z. Li, J. Wan, P. Wang, W. Ding, Z. Fu, Y. Xu, J. Ye, X. Zhang, T. Xie, Z. Cheng, H. Zhang, Z. Yang, H. Xu, and J. Lin, "Qwen2.5-vl technical report," *arXiv preprint arXiv:2502.13923*, 2025.
- [23] Z. Wu, X. Chen, Z. Pan, X. Liu, W. Liu, D. Dai, H. Gao, Y. Ma, C. Wu, B. Wang, Z. Xie, Y. Wu, K. Hu, J. Wang, Y. Sun, Y. Li, Y. Piao, K. Guan, A. Liu, X. Xie, Y. You, K. Dong, X. Yu, H. Zhang, L. Zhao, Y. Wang, and C. Ruan, "Deepseek-vl2: Mixture-of-experts vision-language models for advanced multimodal understanding," 2024. [Online]. Available: <https://arxiv.org/abs/2412.10302>
- [24] Z. Han, C. Gao, J. Liu, J. Zhang, and S. Q. Zhang, "Parameter-efficient fine-tuning for large models: A comprehensive survey," *arXiv preprint arXiv:2403.14608*, 2024.
- [25] P. Sun, H. Kretzschmar, X. Dotiwalla, A. Chouard, V. Patnaik, P. Tsui, J. Guo, Y. Zhou, Y. Chai, B. Caine *et al.*, "Scalability in perception for autonomous driving: Waymo open dataset," in *Proceedings of the IEEE/CVF conference on computer vision and pattern recognition*, 2020, pp. 2446–2454.
- [26] Y. Yao, X. Wang, M. Xu, Z. Pu, Y. Wang, E. Atkins, and D. Crandall, "Dota: unsupervised detection of traffic anomaly in driving videos," *IEEE transactions on pattern analysis and machine intelligence*, 2022.
- [27] Q.-H. Pham, P. Sevestre, R. S. Pahwa, H. Zhan, C. H. Pang, Y. Chen, A. Mustafa, V. Chandrasekhar, and J. Lin, "A3d dataset: Towards autonomous driving in challenging environments," in *Proc. of The International Conference in Robotics and Automation (ICRA)*, 2020.
- [28] A. P. Shah, J.-B. Lamare, T. Nguyen-Anh, and A. Hauptmann, "Cadp: A novel dataset for cctv traffic camera based accident analysis," in *2018 15th IEEE International Conference on Advanced Video and Signal Based Surveillance (AVSS)*. IEEE, 2018, pp. 1–9.
- [29] Y. Li, W. Zhang, K. Chen, Y. Liu, P. Li, R. Gao, L. Hong, M. Tian, X. Zhao, Z. Li *et al.*, "Automated evaluation of large vision-language models on self-driving corner cases," *arXiv preprint arXiv:2404.10595*, 2024.
- [30] W. Bao, Q. Yu, and Y. Kong, "Uncertainty-based traffic accident anticipation with spatio-temporal relational learning," in *ACM Multimedia Conference*, May 2020.
- [31] L. Xu, H. Huang, and J. Liu, "Sutd-trafficqa: A question answering benchmark and an efficient network for video reasoning over traffic events," in *Proceedings of the IEEE/CVF conference on computer vision and pattern recognition*, 2021, pp. 9878–9888.
- [32] C. Parikh, D. Rawat, T. Ghosh, R. K. Sarvadevabhatla *et al.*, "Roadsocial: A diverse videoqa dataset and benchmark for road event understanding from social video narratives," *arXiv preprint arXiv:2503.21459*, 2025.
- [33] Y. Wang, K. Cheng, J. He, Q. Wang, H. Dai, Y. Chen, F. Xia, and Z.-X. Zhang, "Drivingdojo dataset: Advancing interactive and knowledge-enriched driving world model," *Advances in Neural Information Processing Systems*, vol. 37, pp. 13 020–13 034, 2024.
- [34] J. Fang, L.-L. Li, K. Yang, Z. Zheng, J. Xue, and T.-S. Chua, "Cognitive accident prediction in driving scenes: A multimodality benchmark," *arXiv preprint arXiv:2212.09381*, 2022.
- [35] S. Huang, F. Shi, C. Sun, J. Zhong, M. Ning, Y. Yang, Y. Lu, H. Wang, and A. Khajepour, "Drivesotif: Advancing perception sotif through multimodal large language models," *arXiv preprint arXiv:2505.07084*, 2025.
- [36] ByteDance, "Doubao: An intelligent chat assistant by bytedance," 2023, accessed: July 8, 2025.
- [37] P. Wang, L. Li, L. Chen, Z. Cai, D. Zhu, B. Lin, Y. Cao, Q. Liu, T. Liu, and Z. Sui, "Large language models are not fair evaluators," *arXiv preprint arXiv:2305.17926*, 2023.
- [38] Y. Lu, X. Yang, X. Li, X. E. Wang, and W. Y. Wang, "Llmscore: Unveiling the power of large language models in text-to-image synthesis evaluation," *Advances in Neural Information Processing Systems*, vol. 36, pp. 23 075–23 093, 2023.
- [39] B. Li, Y. Zhang, D. Guo, R. Zhang, F. Li, H. Zhang, K. Zhang, P. Zhang, Y. Li, Z. Liu, and C. Li, "Llava-onevision: Easy visual task transfer," 2024. [Online]. Available: <https://arxiv.org/abs/2408.03326>
- [40] A. Marafioti, O. Zohar, M. Farré, M. Noyan, E. Bakouch, P. Cuenca, C. Zakka, L. B. Allal, A. Lozhkov, N. Tazi, V. Srivastav, J. Lochner, H. Larcher, M. Morlon, L. Tunstall, L. von Werra, and T. Wolf, "Smolvlm: Redefining small and efficient multimodal models," *arXiv preprint arXiv:2504.05299*, 2025.
- [41] Y. Zhao, J. Huang, J. Hu, X. Wang, Y. Mao, D. Zhang, Z. Jiang, Z. Wu, B. Ai, A. Wang, W. Zhou, and Y. Chen, "Swift:a scalable lightweight infrastructure for fine-tuning," 2024. [Online]. Available: <https://arxiv.org/abs/2408.05517>